Effects of Reversed-field on Electron Chaotic Orbits in a Free-Electron Laser

Mahdi Esmaeilzadeh[a] and Mohammad S. Fallah[a, b]
[a]Department of Physics, Iran University of Science and Technology, Narmak, Tehran 16844, Iran
[b]Applied–Science Center of Tehran Municipality, No.358,Eskandari St., Tehran, Iran

Abstract—**Chaotic electron dynamics in a free–electron laser with realizable helical wiggler and reversed axial magnetic field is investigated. Poincaré maps are employed to investigate the chaotic electron motion. Numerical calculations show that all trajectories become regular (nonchaotic) for high enough axial magnetic field.**

I. Introduction And Background

A free-electron laser (FEL) is a high-intensity, continuously tunable source of coherent electromagnetic radiation. The radiation is generated by the passage of a relativistic electron beam through a wiggler magnetic field[1]. The electron beam can be collimated by a uniform static axial magnetic field produced by the current in a solenoid. The axial magnetic guide field is often employed in the parallel-field configuration for which the cyclotron rotation of the electron beam is in the same direction as the rotation imposed by the helical wiggler magnetic field. It can also be employed in the reversed-field configuration for which the cyclotron rotation of the electron beam is in the direction opposite to the rotation imposed by the helical wiggler magnetic field. An experimental study shows that the output power and efficiency of the FEL in a reversed-field configuration can be higher than in the parallel-field configuration[2].

The chaotic electron dynamics in ideal and realizable (three-dimensional) helical wigglers in the parallel-field configuration has been studied previosly[3-6]. The present study is an analysis of chaotic electron dynamics in a three-dimensional helical wiggler FEL in the reversed-field configuration

II. Theoretical Model

The motion of an electron in the combined realizable helical wiggler magnetic and reversed axial magnetic fields in the presence of the self–fields may be described by relativistic Hamiltonian

$$H = \{[c\mathbf{P} + e(\mathbf{A}_w + \mathbf{A}_0 + \mathbf{A}_s)]^2 + m^2c^4\}^{1/2} - e\phi_s, \tag{1}$$

where c is the speed of light in vacuum, -e is the electron charge, m is the electron rest mass, γ is the relativistic factor, $\mathbf{P}$ is the canonical momentum,

$$\mathbf{A}_w \equiv \frac{B_w}{k_w}\{[I_0(k_w r) - I_2(k_w r)]\cos\chi\hat{\mathbf{e}}_r - [I_0(k_w r) + I_2(k_w r)]\sin\chi\hat{\mathbf{e}}_\theta\}, \tag{2}$$

is the vector potential for the wiggler magnetic field, $\chi \equiv \theta - k_w z$ and

$$\mathbf{A}_0 \equiv -\frac{1}{2}B_0 r\hat{\mathbf{e}}_\theta \tag{3}$$

is the vector potential for the axial magnetic field. In Eq.(4) $\mathbf{A}_s \equiv \beta_b\phi_s\hat{\mathbf{e}}_z$ is the vector potential for the self–magnetic field, β_b is the average electron axial velocity

$$\phi_s \equiv \frac{m\omega_b^2}{4e}r^2 \tag{4}$$

is the electrostatic potential due to the electron beam, and $\omega_b \equiv (4\pi e^2 n_b / m)^{1/2}$ is the non–relativistic plasma frequency of the electron beam. Since the Hamiltonian (1) is not an explicit function of the normalized time, H is a constant of motion which corresponds to the conservation of total energy. To find an additional constant of motion, the canonical transformation to the new variables (ρ, ψ, ζ, P_ρ, P_ψ, P_ζ) defined by

$$\begin{aligned} &\rho \equiv k_w r, && \psi \equiv \chi, \\ &\zeta \equiv k_w z, && P_\rho \equiv P_r / mc, \\ &P_\psi \equiv k_w P_\theta / mc, && P_\zeta \equiv P_z / mc + k_w P_\theta / mc \end{aligned}$$

is introduced. The normalized Hamiltonian in the new variables can be written as

$$H = mc^2\Big[\Big(\{P_\rho + a_w[I_0(k_w r) - I_2(k_w r)]\cos\psi\}^2 + \left\{\frac{P_\psi}{\rho} - \frac{1}{2}a_0\rho - a_w[I_0(k_w r) + I_2(k_w r)]\sin\psi\right\}^2 + P_z^2/m^2c^2 + 1\Big)^{1/2} - \bar{\phi}_s\Big] \tag{5}$$

where $a_w \equiv eB_w / mk_w c$ is the normalized wiggler magnetic field amplitude, $a_0 \equiv eB_0 / mk_w c$ is the normalized axial magnetic field, $p_z \equiv mc(P_\zeta - P_\psi + \beta_b\bar{\phi}_s)$ is the z component of the mechanical momentum and $\bar{\phi}_s \equiv w_b^2\rho^2 / 4k_w c^2$ is the normalized electrostatic potential due to the electron beam.

978-1-4244-2120-6/08/$25.00 ©IEEE.

Since the Hamiltonian (5) is not an explicit function of ζ, it follows that P_ζ is another constant of motion.

III. Numerical Results ans Discussion

In order to investigate chaotic electron dynamics we use Poincaré maps generated by numerically integrating the equations of motion derived from the Hamiltonian of the system [Eq. (5)]. Figures 1-3 show Poincaré surface–of–section plots in the absence of self-fields for low, medium and high normalized axial magnetic ($a_0 = 1$, 4 and 8), respectively. As we see in Figs. 1 and 2 the phase plane contains chaotic orbits as well as regular (nonchaotic) orbits for low and medium axial magnetic fields. A comparison between Figs. 1 and 2 shows that chaotic orbits decrease with increasing axial magnetic field. The chaotic behavior of electron in the absence of self-fields is due to the spatial inhomogeneity of three-dimensional helical wiggler magnetic field. For high enough normalized axial magnetic field (see Fig. 3) all orbits become regular and nonchaotic. Numerical calculations show that for $a_0 < a_{0T}$ (a_{0T} is the normalized axial magnetic field at which all orbits become regular), the electron motion may be chaotic, while for $a_0 > a_{0T}$ (high axial magnetic field), all trajectories become regular and nonchaotic. The numerical value of a_{0T} at which transition to regular orbits occurs can be computed with the aid of Poincaré surface–of–section plot, which is found to be 4.95 for parameters used in the figures. Numerical calculations show also that the effects of self-fields on electron dynamics cause to increase chaotic trajectories.

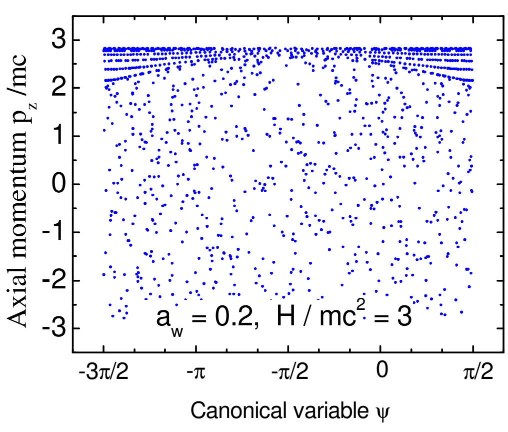

Figure 1. A Poincaré surface–of–section plot in the (ψ, p_z /mc) phase plane for low axial magnetic field ($a_0 = 2$)

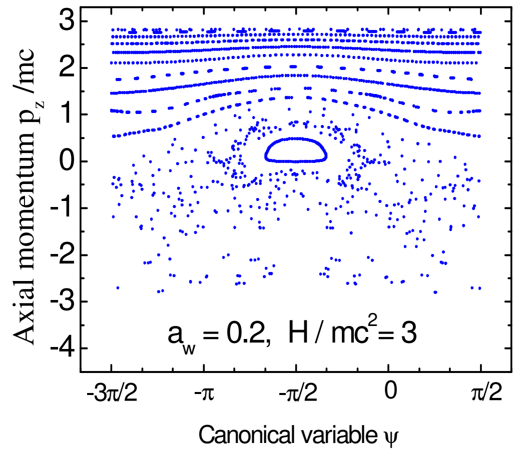

Figure 2. A Poincaré surface–of–section plot in the (ψ, p_z /mc) phase plane for medium axial magnetic field ($a_0 = 4$).

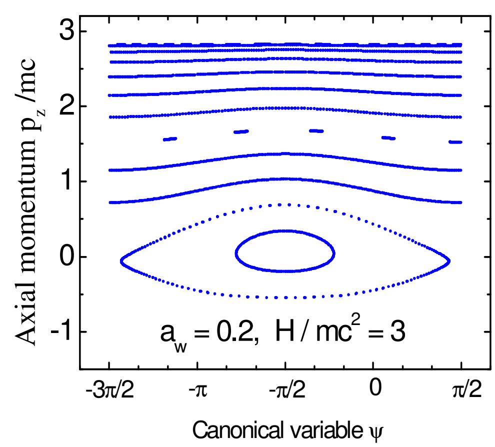

Figure 2. A Poincaré surface–of–section plot in the (ψ, p_z /mc) phase plane for high axial magnetic field ($a_0 = 8$).

References

[1] H. P. Freund and J. M. Antonsen, Jr., *Principles of free electron lasers* (Chapman and Hall, London, 1996).
[2] M. E. Conde and G. Bekefi, Phys. Rev. Lett. **67**, 3082(1991).
[3] C. Chen and R. C. Davidson, Phys. Rev. A **43**, 5541 (1991).
[4] A. Bourdier and L. Michel, Phys. Rev. E **49**, 3353 (1994).
[5] S. K. Nam and K. B. Kim, and E. K. Paik, Nucl. Instr. Meth. A **528**, 56 (2004).
[6] M. Esmaeilzadeh, M. H. Fallah and J. E. Willett, Phys. Plasmas **14**, 013103 (2007).